Detection of apparent skin motion using optical flow analysis: Blood pulsation signal obtained from optical flow sequence

Kazuki Nakajima[a)]
Department of Kansei Design and Engineering, Faculty of Engineering, Yamaguchi University, Tokiwadai, Ube, Yamaguchi 755, Japan

Tsuyoshi Maekawa
Department of Critical Care and Emergency Medicine, School of Medicine, Yamaguchi University, Kogushi, Ube, Yamaguchi 755, Japan

Hidetoshi Miike
Department of Kansei Design and Engineering, Faculty of Engineering, Yamaguchi University, Tokiwadai, Ube, Yamaguchi 755, Japan

(Received 19 June 1996; accepted for publication 11 November 1996)

A skin motion imaging system with two modes of operation, diffusive and specular reflections, was developed. The system consists of image capturing and processing elements. Using optical flow analyses of skin motion at the wrist, we have detected successfully a blood pulsation signal that concurs with the electrocardiogram. The signal provides information not only about blood pulsation, but also about blood circulation and the biomechanical properties of the skin. This system may have other applications in the future, such as noncontact blood pulsation detection and evaluation of the biomechanical properties of skin, for example. © *1997 American Institute of Physics.* [S0034-6748(97)02702-0]

I. INTRODUCTION

Human skin is an elastic tissue that contains pigments, and its mechanical and optical properties are changed by, for example, skin disease and aging. Therefore, during dermatological diagnosis, medical doctors first inspect the stiffness of skin by palpation and the color and luster by observation. It is also known that the surface properties of the skin are sometimes influenced by visceral anomalies and unbalanced body conditions. Thus, medical doctors of many different specialities often pay much attention to the skin of their patients.

To evaluate the surface properties of the skin, several types of equipment have been developed. For instance, the biomechanical impedance measurement system,[1,2] which operates using an artificially forced vibration of the skin, provides information about the biomechanical properties of skin. However, the data produced by such measurements reflect the properties of not only the shallow, but also the deep regions of the skin, and may thus be influenced by the biomechanical properties of internal organs and muscles.

In the work presented here, we describe a system that we have developed for detecting the surface properties of the skin using recently developed optical image processing techniques. From red, green, and blue color images, one may easily evaluate the optical properties of the skin surface. In addition, it is possible to obtain information concerning the biomechanical properties of the skin as well as other new information by using optical flow analysis techniques.[3–5] This is because weak forces induced by the spontaneous activity of the internal organs, such as the pulselike blood flow in arteries and spontaneous excitation and relaxation of muscles, may cause a slight motion of the skin surface.

Initially, we confined ourselves to detecting the optical flow of the skin surface, and found a skin motion that was associated with blood pulsation at the wrist. The blood pulsation signal was detected better when the optical flow analysis was performed on middle-aged subjects, and was barely detectable in young subjects. This age dependence may be associated with the changes in the biomechanical properties of the skin that are caused by aging. The noncontact blood pulsation detected by optical flow analysis appears to be particularly useful in patients with serious burns or violent mental disorders, who are not suitable candidates for ordinary electrocardiogram (ECG) monitoring.

This paper describes a system configuration for skin image capturing and processing and the application of optical flow to skin motion analysis, along with representative data on noncontact cardiac signal detection.

II. THEORY

The optical flow arising from the relative motion of objects and the observer (video camera) is expressed as the

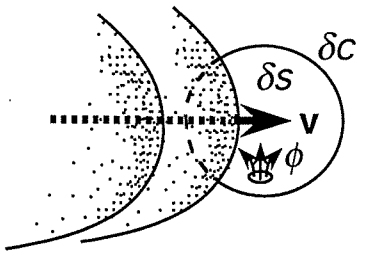

FIG. 1. Graphical representation of the variables of the conservation equation, Eq. (1). A part of a patch moves into a fixed region δs with the motion vector $\mathbf{v}$. δc is the area surrounding of δs, and ϕ is the rate of generation of brightness of the pixels in δs.

a)Author to whom correspondence should be addressed; Electronic mail: naka@sip.eee.yamaguchi-u.ac.jp

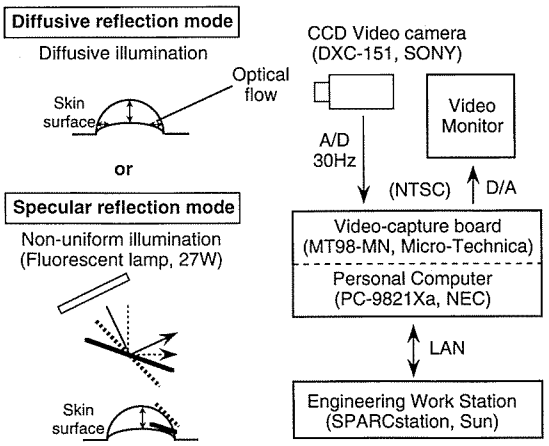

FIG. 2. The skin motion imaging system with its two modes of operation of diffusive and specular reflections.

distribution of apparent velocities of brightness patterns in an image sequence.[3] Consider a temporal change of the brightness in a local area, δs, as shown in Fig. 1. If we define δc as that surrounding the region of interest, δs and $\mathbf{v}=(v_x, v_y)$ as the motion vector (velocity) to be determined, the law of conservation of brightness, f, is represented by the following constraint equation:[5]

$$\frac{\partial f}{\partial t} = -f \text{ div } \mathbf{v} - \mathbf{v} \cdot \text{ grad } f + \phi, \tag{1}$$

where, ϕ is the rate of generation of brightness of pixels in δs. Equation (1) indicates that the temporal change of brightness in δs is caused by both the influx velocities (difference between the influx and the efflux velocities) and the rate of generation of brightness in δs. If div $\mathbf{v}=0$ and $\phi=0$, Eq. (1) is reduced to the well-known basic constraint equation:[3]

$$\frac{\partial f}{\partial t} = -\mathbf{v} \cdot \text{ grad } f. \tag{2}$$

The conditions of div $\mathbf{v}=0$ and $\phi=0$ require motion of a rigid body, constancy, and uniformity of illumination, and the object motion to be perpendicular to the optical axis of the camera.

In the study reported here, we assume simply that div $\mathbf{v}=0$ and $\phi=0$ in determining the optical flow for reducing both the number of uncertain variables and computation time, although the deformability of the skin surface and nonuniform illumination meant that div $\mathbf{v}\neq 0$ and $\phi\neq 0$. A detailed calculation procedure is described in the literature.[4,5]

III. INSTRUMENT AND EXPERIMENTAL PROCEDURE

Figure 2 shows a schematic diagram of the skin motion imaging system with its two operational modes of diffusive and specular reflections. The video camera was placed at a distance of 1 m from an object. The image of the object was zoomed until it was a suitable size for optical flow analysis, and then the skin images were digitized, frame to frame, at a rate of 30 frames per second using a personal computer equipped with a video-capture board. The obtained image data were uploaded to a SUN work station and processed to obtain optical flow fields. The software used for sequential image acquisition and image data processing was developed by our research group.[4,6] An ECG was recorded simultaneously using an ECG monitor (CM_5 lead; Dyna scope DS-3100, Fukuda Denshi) at 250 Hz.

TABLE I. Results of the eye inspection. D: diffusive reflection, and S: specular reflection.

	Apparent skin motion				
	+			−	
Age	D	S	D+S	S	Subtotal
20–29	2	4	6	18	24 [a]
30–39	6	0	6	3	9 [a] [a]
40–49	3	2	5	4	9
Total	11	6	17	25	42

[a] $P<0.01$ (exact probability test).

In the diffusive reflection mode, the optical flow of the translational motion of objects can be detected. The specular reflection mode is suitable for the detection of changes in the inclination of the object.[7] Thus, the specular reflection mode is more sensitive in detecting weak skin motion. To obtain specular reflection images, the skin surface was coated with an oily layer of a gel ointment normally used for skin care (Oronaine®H ointment, Otsuka Seiyaku). Ceiling and desktop-type fluorescent lamps were used as the illumination light sources for the diffusive and specular reflection modes, respectively.

The skin motion at the wrist of 42 healthy volunteers was inspected by eye under both diffusive and specular reflection modes prior to experiments. Table I gives the results of the eye inspection. The skin motion due to cardiac pulse was hardly visible in young subjects, but was easily observed in some of the middle-aged subjects. Skin motion was detected in 11 subjects using the diffusive reflection mode. When using the specular reflection mode, skin motion was detected for six more subjects. We confirmed a significant difference between the young and middle-aged subject groups using a statistical exact probability test[8] ($P<0.01$). Image measurements and optical flow analyses were only carried out for the 17 volunteers who exhibited apparent skin motion when they were in a supine posture.

IV. RESULTS

A. Optical flow field of blood pulsation signal

A typical result obtained using the diffusive reflection mode on a 33-year-old male is shown in Fig. 3, which shows a view of the left wrist together with the associated optical flow fields. The skin motion associated with cardiac activity is observed clearly as two-dimensional motion vectors. The direction of the motion vectors around the radial artery is perpendicular to the artery. Figure 4 shows a model of skin motion associated with the arterial vibration caused by a cardiac pulse. The observed optical flow distribution (see Fig. 3) corresponds roughly to this model. The deformability of the skin surface does not necessarily satisfy the assumption of

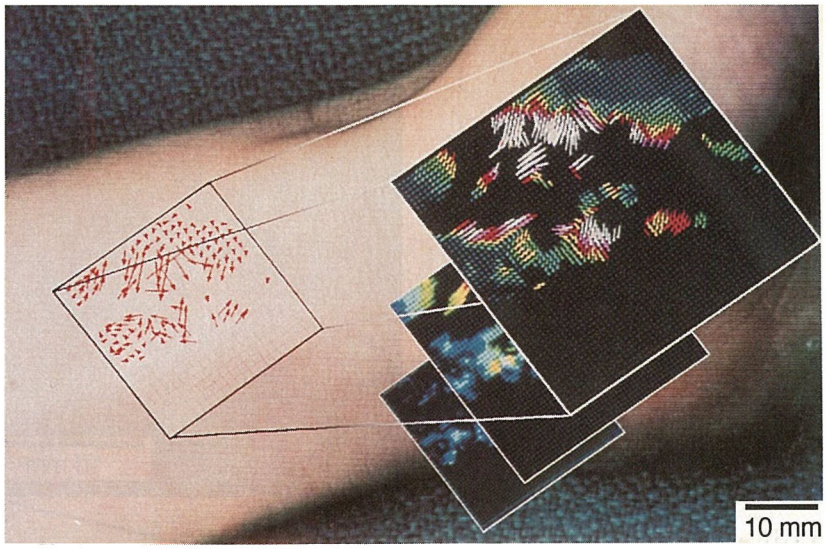

FIG. 3. A view of the left wrist of a healthy volunteer. The palm and elbow are located in the upper-right and the lower-left corners, respectively. The transparent square window shows the location of the captured image (64×64 pixels in size). A sequence of three analyzed optical flow fields are superimposed.

div $\mathbf{v}=0$ and $\phi=0$, as described in the previous section. However, our assumption is still usable for the quantitative evaluation of skin motion.

A series of optical flow fields are shown in Fig. 5. The temporal series of the optical flow fields around the artery are classified into two categories: one is the dynamic phase, which has large motion vectors ($\geqslant$0.4 pixels/frame), and the other is the static phase, which has no appreciable vectors. The dynamic phase arose in seven image frames (red underlined) at 0.10–0.30 s and another seven frames at 1.00–1.20 s. The static phase occurred in another 20 frames at 0.33–0.97 s. Thus, the periodic behavior of the optical flow fields became apparent. The period of the dynamic phase is 0.23 s. Considering the fact that the typical cardiac systolic period continues for 0.2–0.3 s,[9] it may be concluded that the dynamic phase is due to the systolic phase.

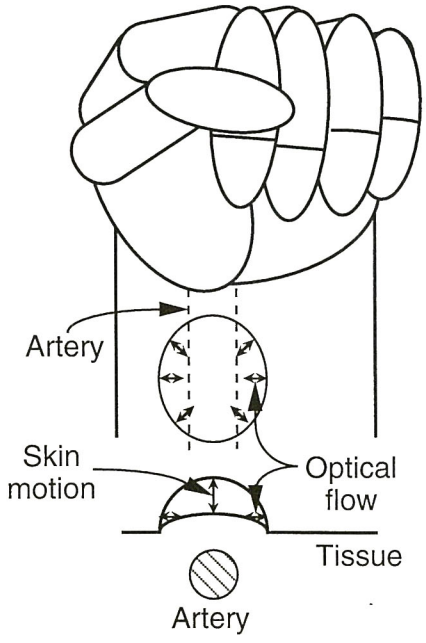

FIG. 4. A model for skin motion. The expansion or contraction of the radial artery causes mechanical stress of the tissue and optical flow arises due to the skin motion.

B. Analysis of the optical flow field for blood pulsation detection

We detected motion vectors in a local area above the radial artery. To detect the blood pulsation signal from the optical flow fields, we introduced a new variable, ''local area divergence (LAD),'' defined by

$$\mathrm{LAD}\equiv\int_{\delta s}\mathrm{div}\ \mathbf{v}\,ds=\oint_{\delta c}\mathbf{v}\cdot\mathbf{n}\,dc. \tag{3}$$

LAD was calculated for a square within the target area, and was compared with the mean velocity $\langle\mathbf{v}\rangle$ evaluated from the same local area for LAD calculation, and with an ordinary evaluation function of difference image $D(t)$. Details of calculations for LAD, $\langle\mathbf{v}\rangle$ and $D(t)$ are described in the Appendix.

Figure 6 shows the wave forms of LAD, $\langle\mathbf{v}\rangle$ and $D(t)$. The interval between the two nearest large peaks agrees well with the $R-R$ interval of the ECG. An approximately 200-ms time lag was observed between the LAD wave and the ECG. This value agrees well with the delay of the blood flow pulse transition to the wrist.[10] The LAD shows positive and negative peaks corresponding to the expansion and contraction, respectively, of the wrist artery. It also exhibits a dull response to changing the size of the local area δs (see Fig. 7). All wave forms exhibit nearly the same behavior. However, $\langle\mathbf{v}\rangle$ always has a positive value because $\langle\mathbf{v}\rangle$ is the norm of the motion vectors and has no directional information. The wave form of $D(t)$ is always noisy. We emphasize that $D(t)$ exhibits poor robustness but that LAD and $\langle\mathbf{v}\rangle$ are more reliable, as shown in Fig. 6.

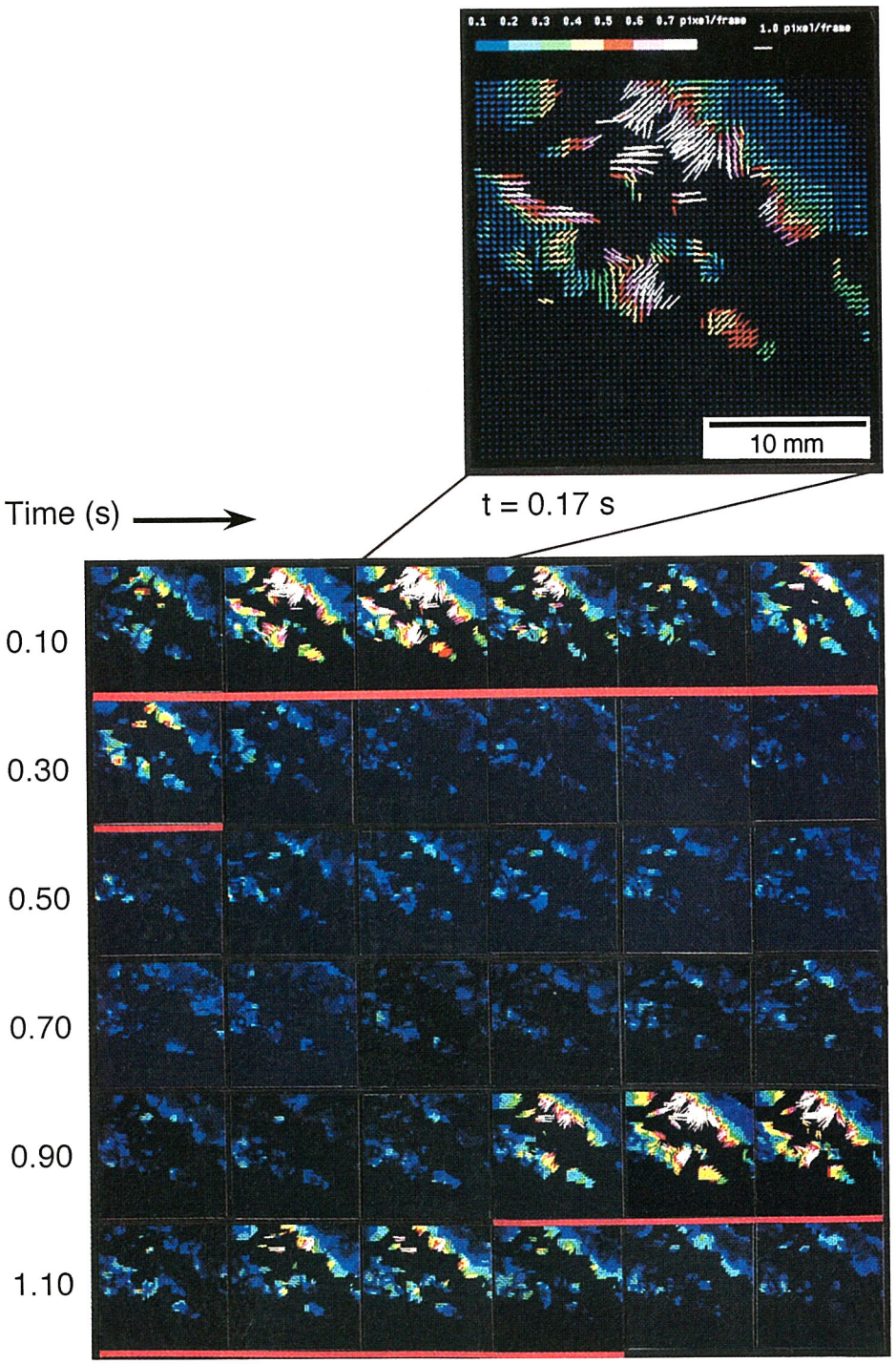

FIG. 5. Motion vector (optical flow) fields obtained using the gradient-based method. The motion vectors are indicated by dots and bars.

C. Specular and diffusive reflection images

For weak skin motion, it was rather difficult to detect the blood pulsation signal in the diffusive reflection mode. Figure 8 shows a typical result of LAD and $\langle \mathbf{v} \rangle$ obtained from the data obtained using the specular and diffusive reflection modes. The blood pulsation signal was detected clearly in the specular reflection mode [Fig. 8(A)] but not in the diffusive mode [Fig. 8(B)]. We obtained a better signal-to-noise ratio in LAD, and the blood pulsation cycle of LAD was clearer than that of $\langle \mathbf{v} \rangle$, as shown in Fig. 8(A). The power spectrum of LAD obtained in the specular reflection mode exhibits sharp peaks [Fig. 8(C)], whereas those of the diffusive mode are broad [Fig. 8(D)]. The frequency of one of the peaks agrees well with the frequency of the heart beat, which is marked by a bold arrow.

V. DISCUSSION

As described in Sec. IV, we have detected successfully a blood pulsation signal using optical flow analysis of skin motion. However, in the case of young subjects and some of

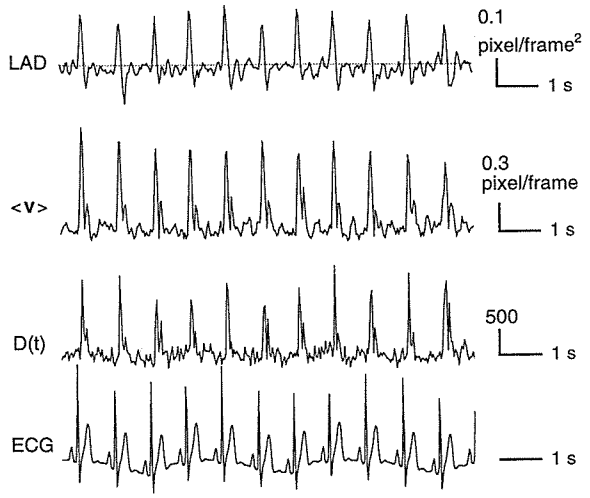

FIG. 6. The wave forms of LAD ($\delta s = 17 \times 17$ pixels), $\langle \mathbf{v} \rangle$ and $D(t)$ obtained from the data taken obtained using the diffusive reflection modes. LAD and $\langle \mathbf{v} \rangle$ were evaluated by the velocity of the motion fields in Fig. 5. $D(t)$ was calculated from the law image sequence. The dashed lines indicate the zero level of LAD. The ECG was recorded simultaneously.

the middle-aged subjects, it was hard to detect the blood pulsation signal, even using the specular reflection mode.

As shown in Fig. 4, the expansion or contraction of the artery caused a mechanical stress on the skin in contact with the artery. This mechanical stress propagates to, and gives rise to deformation of the skin surface. If we consider such a simple mechanism, the degree of skin surface deformation depends upon: (1) the magnitude of stress caused by artery expansion and contraction, (2) the depth of the artery from the skin surface, and (3) the biomechanical properties of the skin (e.g., softness or skin surface tension).

The magnitude of stress caused is dependent upon the blood ejection from the heart and the hardness of the artery. In our experiments, we found that the blood pulsation signal was detected better when measuring the subjects soon after doing physical exercise and/or eating. Thus, cardiac activity affects the blood pulsation signal intensity. In general, the hardness of arteries increases with age, and arteriosclerosis may suppress artery expansion due to blood flow. Some of the middle-aged subjects in whom no appreciable blood pulsation signal was obtained might have had symptoms of arteriosclerosis or related troubles, although unfortunately we did not have medical diagnosis data for those subjects.

The depth of the artery was estimated from the data of

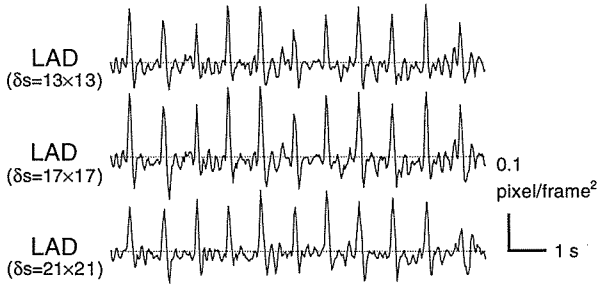

FIG. 7. Influence of changes in the local area δs on the evaluation of LAD. LAD waves were evaluated from the same motion field sequences as shown in Fig. 5. The dashed lines indicate the zero level of LAD.

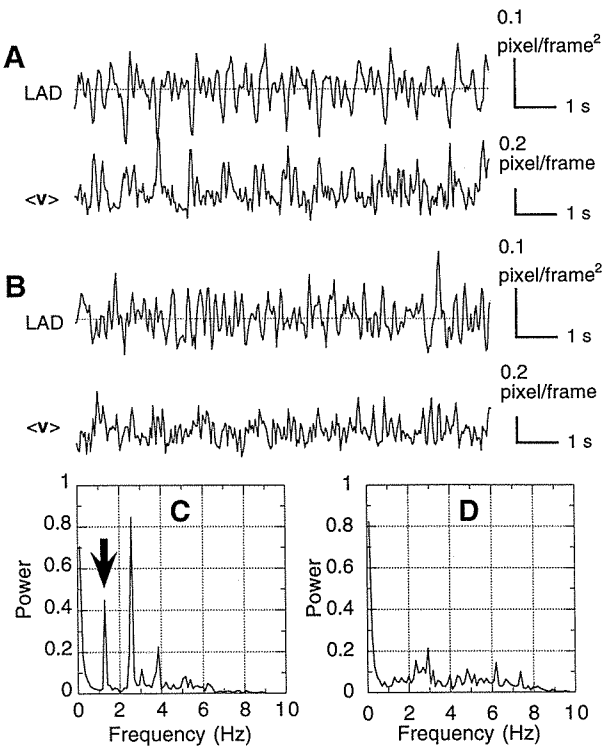

FIG. 8. LAD ($\delta s = 25 \times 25$ pixels) and $\langle \mathbf{v} \rangle$ obtained from the optical flow data. Wave forms obtained from the data obtained using (A) the specular and (B) the diffusive reflection modes, respectively, of the right wrist of a 23-year-old male. The dashed line indicates the zero level of LAD. Power spectra (C) and (D) were obtained from LADs (A) and (B), respectively. In spectrum (C), the peak marked by the bold arrow agrees well with the averaged heart rate of the subject (1.29 Hz=77 b.p.m.), and harmonics are visible at 2.58 and 3.87 Hz.

body weight and stature. Except for extremely heavy subjects, we found no clear correlation between weight and the blood pulsation signal intensity. Thus, the depth of the artery does not appear to be important for the detection of a blood pulsation signal in normal subjects.

Skin elasticity usually decreases with age, and skin surface tension decreases steeply after the age of 20–24 years. The absence of a blood pulsation signal in any of the young subject suggests strongly the importance of such biomechanical factors for the appearance of a blood pulsation signal. We think, therefore, that the significant difference in the blood pulsation signal intensity obtained for the two groups of subjects, young and middle aged, is probably due to the degradation of skin elasticity and skin surface tension caused by aging in the latter.

We conclude that the blood pulsation signal contains information not only about blood pulsation, but also about blood circulation and the biomechanical properties of skin. LAD and $\langle \mathbf{v} \rangle$ are better than $D(t)$ for extracting the blood pulsation signal.

The ECG is widely used for monitoring the heart beat signal. However, in several restricted cases, e.g., patients with serious burns or mental disorders, the ECG is not easily usable. From the viewpoint of clinical applications, the noncontact blood pulsation detection system utilizing optical flow analysis may be useful in such cases.

In conclusion, we have developed a highly sensitive skin

motion monitoring system and found that the blood pulsation signal is detectable using optical flow analyses. We emphasize that this system may have other applications, such as noncontact blood pulsation detection and evaluation of the biomechanical properties of the skin.

ACKNOWLEDGMENTS

The authors are grateful to Professor D. Sadamitsu, Dr. K. Nakashima, and Professor T. Tamura for discussions, and to Dr. A. Nomura for helpful comments. Thanks are also due to Mr. A. Osa for his help with the experiments. This work was partly supported by the Terumo Life Science Foundation and Welfare Techno-House Ube of the Japanese Agency of Industrial Science and Technology Ministry of International Trade and Industry.

APPENDIX

LAD was evaluated for a local square δs (e.g., $w \times w$ pixels) around the center, $\mathbf{v}(x,y)$, of a velocity field. Then LAD was represented by the following equation:

$$\mathrm{LAD} \equiv \sum_{k=w/2}^{w/2} m \times v_x\left(x+\frac{w}{2}, y+k\right) - \sum_{k=w/2}^{w/2} m \times v_x\left(x-\frac{w}{2}, y+k\right) + \sum_{k=w/2}^{w/2} m \times v_y\left(x+k, y+\frac{w}{2}\right) - \sum_{k=-w/2}^{w/2} m \times v_y\left(x+k, y-\frac{w}{2}\right),$$

$$w \geq 3 \text{(an odd number)}, \quad \left\{ \begin{array}{l} m=1,\ k=\dfrac{w}{2}, -\dfrac{w}{2} \\ m=2,\ k \neq \dfrac{w}{2}, -\dfrac{w}{2} \end{array} \right\}. \tag{A1}$$

The mean velocity of an optical flow field $\langle \mathbf{v} \rangle$ is obtained as follows:

$$\langle \mathbf{v} \rangle = \sum_x \sum_y \sqrt{v_x^2 + v_y^2}/A_w. \tag{A2}$$

Here, v_x and v_y are the respective components of the motion vector and A_w is the same local square δs as used for the LAD calculation.

The value of $D(t)$ is defined as an ordinary evaluating function,

$$D(t) = \sum_x \sum_y |f(x,y,t) - f(x,y,t-1)|, \tag{A3}$$

where $f(x,y,t)$ is an image function (brightness distribution) at coordinates (x,y) and time t.

[1] H. Oka and T. Yamamoto, Med. Biol. Eng. Comput. **21**, 778 (1983).
[2] H. Oka and T. Yamamoto, Trans. IECE Jpn. **E67**, 49 (1984).
[3] K. P. Horn and G. S. Schunck, Artif. Intell. **17**, 185 (1981).
[4] H. Miike, K. Koga, H. Hashimoto, M. Momota, and A. Nomura, *Pasokon Niyoru Dogazo Shori; Image Sequence Processing by Microcomputer*, edited by H. Miike and K. Koga (Morikita, Tokyo, 1993) (in Japanese).
[5] A. Nomura, H. Miike, and K. Koga, Pat. Recog. Lett. **16**, 285 (1995).
[6] K. Nakajima, A. Osa, S. Kasaoka, K. Nakashima, T. Maekawa, T. Tamura, and H. Miike, Jpn. J. Appl. Phys. 2 **35**, L269 (1996).
[7] H. Miike, K. Koga, T. Yamada, T. Kawamura, M. Kitou, and N. Takikawa, Jpn. J. Appl. Phys. 2 **34**, L1625 (1995).
[8] T. D. V. Swinscow, in *Statistics at Square One* (British Medical Journal London, 1976), Chap. 9 [Japanese translation: edited by Tokei-shori, K. Nishimura, translated by K. Ohoshima (Kyoritsu, Tokyo, 1982)].
[9] A. P. Yoganathan, J. Hopmeyer, and R. S. Heinrich, in *The Biomedical Engineering Handbook*, edited by J. D. Bronzino (Chemical Rubber, FL, 1995), Chap. 32, p. 440.
[10] K. Nakajima, T. Tamura, and H. Miike, Med. Eng. Phys. **18**, 365 (1996).